

Glyco-Modification of Mucin Hydrogels to Investigate Their Immune Activity

Hongji Yan, Morgan Hjorth, Benjamin Winkeljann, Illia Dobryden, Oliver Lieleg, and Thomas Crouzier*



Cite This: *ACS Appl. Mater. Interfaces* 2020, 12, 19324–19336



Read Online

ACCESS |



Metrics & More



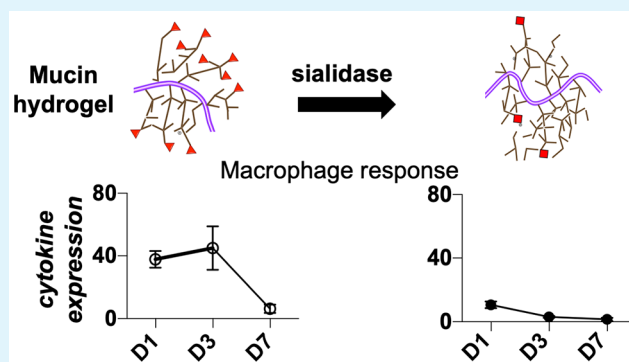
Article Recommendations



Supporting Information

ABSTRACT: Mucins are multifunctional glycosylated proteins that are increasingly investigated as building blocks of novel biomaterials. An attractive feature is their ability to modulate the immune response, in part by engaging with sialic acid binding receptors on immune cells. Once assembled into hydrogels, bovine submaxillary mucins (Muc gels) were shown to modulate the recruitment and activation of immune cells and avoid fibrous encapsulation *in vivo*. However, nothing is known about the early immune response to Muc gels. This study characterizes the response of macrophages, important orchestrators of the material-mediated immune response, over the first 7 days in contact with Muc gels. The role of mucin-bound sialic acid sugar residues was investigated by first enzymatically cleaving the sugar and then assembling the mucin variants into covalently cross-linked hydrogels with rheological and surface nanomechanical properties similar to nonmodified Muc gels. Results with THP-1 and human primary peripheral blood monocytes derived macrophages showed that Muc gels transiently activate the expression of both pro-inflammatory and anti-inflammatory cytokines and cell surface markers, for most makers with a maximum on the first day and loss of the effect after 7 days. The activation was sialic acid-dependent for a majority of the markers followed. The pattern of gene expression, protein expression, and functional measurements did not strictly correspond to M1 or M2 macrophage phenotypes. This study highlights the complex early events in macrophage activation in contact with mucin materials and the importance of sialic acid residues in such a response. The enzymatic glyco-modulation of Muc gels appears as a useful tool to help understand the biological functions of specific glycans on mucins which can further inform on their use in various biomedical applications.

KEYWORDS: mucin hydrogels, glyco-modulation, surface nanomechanical property, macrophages, sialic acid



INTRODUCTION

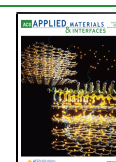
Breakthroughs in materials engineering have accelerated the use of biomaterials in both preclinical and clinical applications, including engineered cell microenvironments,^{1–3} drug delivery,⁴ tissue engineering,⁵ and immunoengineering.⁶ A new class of biomaterials has emerged that is not designed to be “biologically inert” but rather to deliver a provision of cues to surrounding cells resulting in improved material performance.⁷ This approach is particularly valuable when considering that the immune response to implanted biomaterials can help suppress or modulate the immune cascades to avoid acute inflammation or subacute inflammation. These materials find applications in regenerative medicine, where hyperactivity of immune cells in a damaged tissue is suppressed by the material to promote the healing process,⁸ or in cancer therapy⁹ and novel vaccine therapies,¹⁰ where a complex immune-modulation from the material can help eradicate diseased cells and promote healthy cells *via* a myriad of coordinated intra- and extracellular signaling pathways.

Mucin glycoproteins are emerging as attractive building blocks to assemble such bioactive materials,^{11,12} driven by advances in our understanding of their structure and biological functions. Mucins are a family of glycosylated proteins, and up to 80% of their mass is composed of O-glycans. Mucins are found bound to the cell membrane as part of the glycocalyx^{13,14} or secreted to form the mucus gel protecting the epithelium against irritants and pathogens and to provide hydration and lubrication.^{11,15} In addition to the physical protective role, mucins have also recently appeared as very bioactive molecules. Mucins are immunologically active through the binding of their sugar residues to lectin-like proteins on the surface of immune cells.^{15,16} The muc2 mucins found in the gut can imprint

Received: February 25, 2020

Accepted: April 3, 2020

Published: April 17, 2020



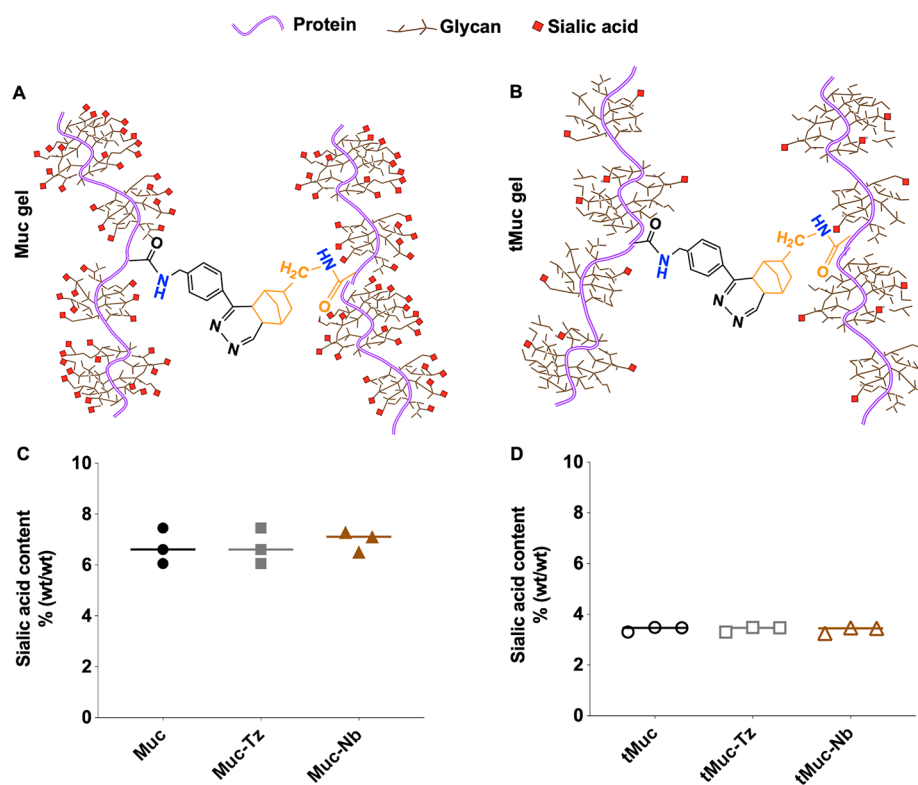


Figure 1. Muc gels cross-linking reaction and mucin glycan modification. Representation of the cross-linking reaction of Muc gels (A) and tMuc gels (B, neuraminidase-treated). Quantification of sialic acid residues on Muc, Muc-Tz, and Muc-Nb (C) and neuraminidase-treated tMuc, tMuc-Tz, and tMuc-Nb (D). The data points are obtained from measurements of $n = 3$ independent samples.

dendritic cells tolerance¹⁶ and, in contrast, can activate nonstimulated dendritic cells in a concentration-dependent manner.¹⁷ In mucinous carcinomas, secreted mucins surround the tumors protecting them from cancer drugs and immune cell infiltration both physically and biochemically.¹⁸ Inoue *et al.* reported that bovine submaxillary mucins supplemented in cell culture medium could activate IL1b expression in macrophages derived from the human THP-1 monocyte cell line (THP-1-M0) in a sialic acid-dependent manner.¹⁹

The evidence for a broad range of bioactivities of mucins, and in particular their immune-modulating activities, has prompted us to investigate whether mucins could be assembled into immune-modulating biomaterials. Biomaterials able to orchestrate the immune reaction to their implantation could be the key to overcome long-standing challenges in biomaterial science, including chronic inflammatory and fibrotic encapsulation.²⁰ We have recently shown that covalently cross-linked mucin hydrogels (Muc gels) made of bovine submaxillary mucins (Muc) modulate the foreign body response *in vivo*. Those hydrogels caused a broad-dampening effect of cytokine expression in macrophages harvested from the explanted gels and their corresponding peritoneal cavity, and the absence of fibrous encapsulation after 21 days.²¹ This discovery suggests that biomaterials containing mucins or mucin-like molecules could be used as implantable hydrogels and coatings that can evade fibrosis and ensure the long-term function of the devices. However, fibrous capsule formation is typically initiated after ~2 weeks of implantation,²¹ and the earlier events that led to such effects are unknown. In addition, none of the features of mucins essential for their immune-modulating properties were clearly identified.

We address these limitations herein by investigating the response of undifferentiated macrophages (M0s) derived from monocyte cell line THP-1 and human primary peripheral blood monocytes when cultured on the surface of Muc and tMuc gels (glyco-modulated Muc gels) over 7 days. The tMuc gels are used to highlight the role of mucin-bound sialic acid residues in the immune-modulating effect. We focus the study on macrophages since material–immune interactions are predominantly orchestrated by macrophages *in vivo*, owing to their heterogeneity and plasticity.⁷ Unlike other terminally differentiated cells, macrophages can sense cues from their environment and undergo dynamic changes,²² either fighting against pathogens⁷ or contributing to tissue healing *via* directing stromal cell recruitment and differentiation to maintain tissue homeostasis.²² In cancers, tumor-associated macrophages (TAMs) are polarized toward a pro-tumoral phenotype contributing to a tumor immunosuppressive microenvironment.²³ In some cancers, mucins can contribute to their pro-tumoral polarization, for instance in the lung, where MUC5B mucins were shown to directly impact TAM phenotype.²⁴ Thus, by studying macrophage reaction to Muc gels, we characterize an important component of the immune reaction these materials would elicit *in vivo*.

RESULTS

Glycan Composition of Muc Gels can be Modulated by Enzymatic Treatment without Compromising the Mechanical Properties of the Gels. To prepare mucin hydrogels (Muc gels), we introduced tetrazine (Tz) and norbornene (Nb) functionalities to bovine submaxillary mucin (Muc) molecules as previously described.²¹ After being mixed in solution, Muc-Tz and Muc-Nb formed a covalently cross-linked hydrogel through

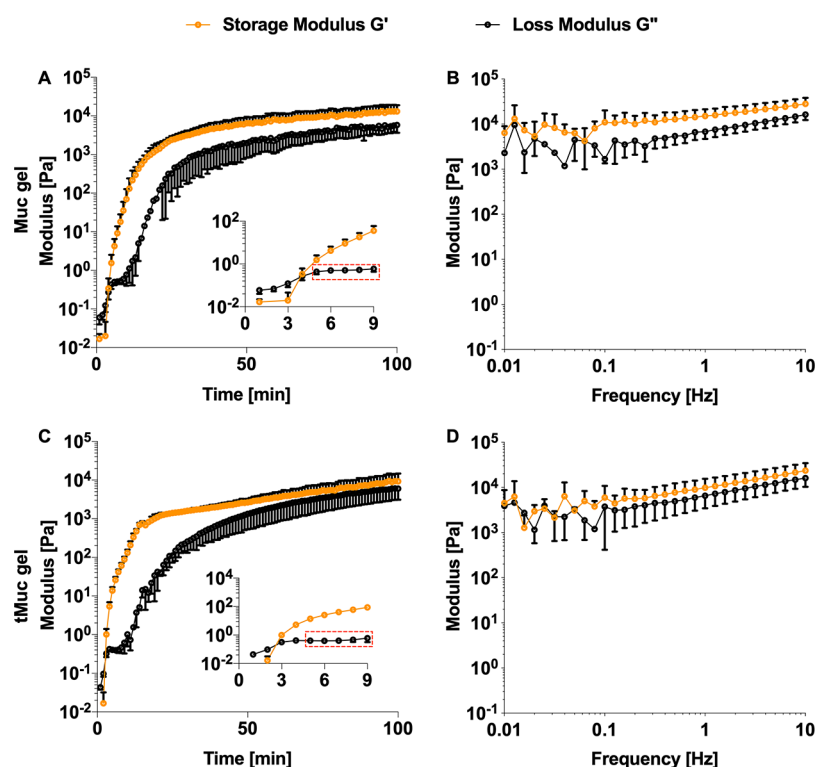


Figure 2. Rheological characterization of Muc gels and tMuc gels. Time-dependent rheological measurements of the mixed Muc-Tz and Muc-Nb (A) or tMuc-Tz and tMuc-Nb (C) in PBS. Final frequency-dependent viscoelastic moduli of the cross-linked Muc-gel (B) and tMuc gels (D). The error bars denote the standard deviations as obtained from measurements of $n = 3$ independent samples.

an inverse electron demand Diels–Alder cycloaddition reaction (Figure 1A,B). To investigate the role of sialic acid in the response of macrophages, we cleaved sialic acid residues by treating Muc-Tz (tMuc-Tz) and Muc-Nb (tMuc-Nb) with neuraminidase (Figure 1B). We show by anion exchange chromatography that about 60% of all sialic acid residues were removed after neuraminidase treatment (Figure 1C,D). This incomplete removal of sialic acid could be due to the inaccessibility of a fraction of the sialic acid residues or to the specificity of the neuraminidase used. However, given that we obtained an even removal efficiency for the modified and unmodified mucins, the presence of Tz and Nb, which we hypothesize to be located on the mucin protein backbone (Supporting Information Figure S1), does not seem to be responsible for this incomplete sialic acid removal.

We then tested whether the enzymatic treatment would compromise the rheological properties of the hydrogels; such an effect could influence the macrophage response to the material²⁵ and make the contributions of sialic acid difficult to infer. Muc-Tz and Muc-Nb solubilized in PBS were mixed and then subjected to oscillatory rheology measurements over time. Both the loss (G'') and storage (G') moduli rapidly increased, and initially the response was dominated by G'' (indicating the presence of a viscoelastic solution) (Figure 2A). However, ~ 5 min after mixing, the response became dominated by G' , indicating the presence of a viscoelastic solid thus confirming successful gel formation (Figure 2A, insert). Both storage and loss modulus reached a plateau-like state after ~ 60 min. This plateau value of G' was ~ 10 kPa, which is several orders of magnitude higher than the elastic modulus of an un-cross-linked, entangled mucin solution.²⁶ A frequency sweep performed after the viscoelastic moduli have reached plateaus demonstrated that the system appears indeed to be efficiently and covalently cross-

linked (Figure 2B). Gels with similar viscoelastic properties were obtained when using a complete cell culture medium to dissolve the mucins, suggesting the medium did not interfere with the cross-linking reactions occurring between Tz and Nb (Figure S2). Importantly, neuraminidase-treated tMuc-Tz and tMuc-Nb also reacted to form hydrogels and showed a rheological behavior and calculated mesh size⁵ (ξ) similar to those of untreated Muc gels (Figure 2C(insert),D; Table 1). With an average of 11.6 kPa, the average elastic modulus of tMuc gels was 1 kPa lower than Muc gels but with no statistical difference ($p = 0.09$).

Table 1. Mesh Size Values Estimated from the Rheology Data Shown in Figure 2 ($n = 3$)

sample	ξ (nm)	$p = 0.435$
Muc gel	7.14 ± 1.13	
tMuc gel	8.31 ± 1.71	

We further characterized the nanomechanical surface properties of hydrated Muc gels and tMuc gels by atomic force microscopy (AFM) based nanomechanical surface mapping with the tip submerged in PBS. The measurement is complementary to the bulk rheometer measurements and allows us to reveal the surface heterogeneity in nanomechanics in a range of the AFM tip's radius.²⁷ We recorded force volume maps for both approach (a combined elastic and viscous contribution) and retraction regimes (mainly elastic contributions). The average elastic modulus (Figure 3A,B) calculated from the elastic modulus maps (Figures S3 and S4) showed no difference between Muc gels and tMuc gels. There was also no difference in the stiffness (Figure 3C,D) calculated from the

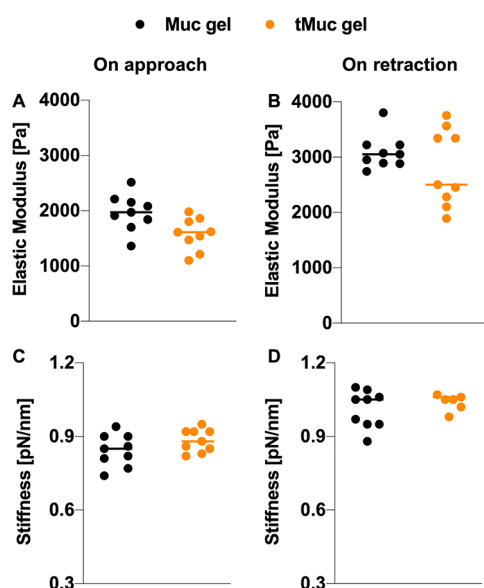


Figure 3. AFM nanomechanical characterization of Muc gels and tMuc gels. Elastic moduli (A, B) and stiffness (C, D) of Muc gels and tMuc gels were obtained by AFM-based force volume mapping for both approach (elastic, viscous, and viscoelastic contributions) and retraction regimes (mainly elastic contribution). $n = 9$.

slopes in the repulsive part of the force curves, which are independent of contact models.²⁸

The Phagocytic Ability of THP-1-M0 is Decreased When Cultured on Muc Gels but not Their Endocytotic Ability. To investigate the early response of macrophages to mucin materials, we first used macrophages type 0 differentiated from human monocyte cell line THP-1 (THP-1-M0) by incubation with phorbol 12-myristate 13-acetate (PMA, 150 nM) for 3 days followed by incubation in a complete cell culture medium without PMA for 1 day. After differentiation, the cells became adherent to tissue culture polystyrene (TCP) and

expressed increased levels of CD36 and CD71 macrophage markers²⁹ compared to THP-1 monocytes (Figure S5). We seeded THP-1-M0 on tissue culture polystyrene (TCP), Muc gel, and tMuc gels and cultured them over a period of 7 days. THP-1-M0 did not adhere strongly, did not spread, and formed clusters within hours on both Muc gels and tMuc gels (Figure 4). As expected, the differentiated THP-1-M0 cultured on Muc gel and tMuc gel did not proliferate as suggested by unchanged metabolic activity from day 0 to 7 (Figure S6). This suggests that changes in the gene expression profile in THP-1-M0 were not due to significant changes in cell viability.

We then ask whether undifferentiated M0 macrophages would be activated and be polarized when in contact with Muc gels. Historically, macrophages have been broadly classified into pro-inflammatory phenotype (M1) that is stimulated by pro-inflammatory signals, such as interferon- γ (IFN- γ) or microbial products lipopolysaccharide (LPS),³⁰ and alternatively activated (M2) that is stimulated by signals from basophils, mast cells, and other granulocytes, or interleukin 4 and interleukin 13 (IL4 and IL13).³⁰ M1 cells have higher capacity in antigen-presenting, and enhancing Th1 differentiation of lymphocytes that produces the pro-inflammatory signals.^{30,31} M1 cells also harm adjacent cells *via* producing toxic reactive oxygen species (ROS) and escalating the pro-inflammatory responses.³² M2 also constantly expresses scavenger and mannose receptors and releases anti-inflammatory cytokines, *i.e.*, IL-10.³⁰

We measured the gene expression of 11 pro- and anti-inflammatory macrophages markers by RT-PCR (Tables S1 and S2). There was no significant difference in expression of the majority of markers over 7 days between nonadhesive and adhesive TCP (Figure S7) but with a slight activation of THP-1-M0 for some cytokines (*i.e.*, *CXCL10*, *CXCL8*, and *CCL2*) on adhesive TCP. We thus selected adherent TCP as reference material even though M0 macrophages adhere to TCP and not Muc gels. Both pro-inflammatory *CXCL10*, *CXCL8*, *TNFA*, *CCL2*, *IL1B*, *VEGFA* and anti-inflammatory *IL1Ra* cytokines were upregulated on the first day, then followed by a decrease on

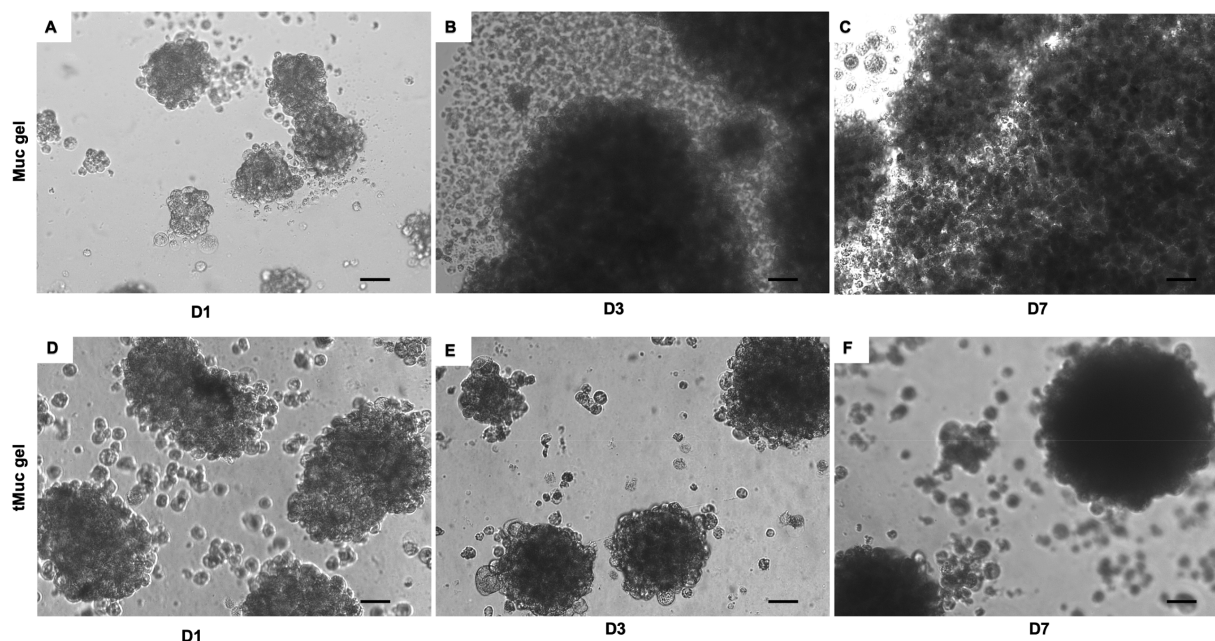


Figure 4. Representatives of phase-contrast images of THP-1-M0 cultured on Muc gel and tMuc gel on days 1, 3, and 7 (D1, D3, and D7). Scale bar = 50 μm .

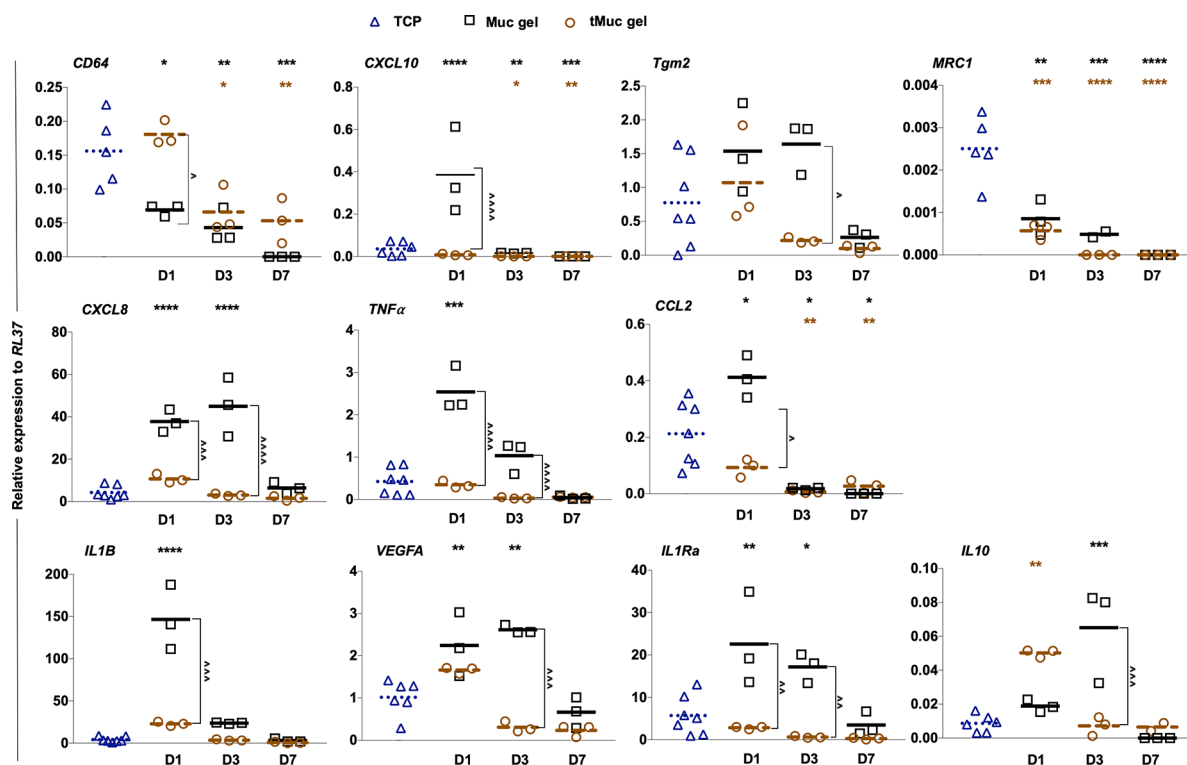


Figure 5. Gene expression in THP-1-derived macrophages type 0 (THP-1-M0) after being cultured on tissue culture polystyrene (TCP), Muc gels, and sialidase-treated Muc gels (tMuc gel) on D1, D3, and D7. The data points denote the mean of relative gene expression to RPL-37 obtained from three independent experiments with duplicates. Statistical significance was calculated by one-way ANOVA test by Prism 8.0. Black *, brown *, and black ^ indicate the comparison between Muc gels vs TCP, tMuc gels vs TCP, and Muc gel vs tMuc gel, respectively. *, **, ***, and **** indicate *p* values of <0.05, 0.01, 0.0005, and 0.0001, respectively.

days 3 and 7 in THP-1-M0 cultured on Muc gels when compared to TCP and tMuc gels, except for *CXCL8*, *VEGFA*, and *IL1Ra*, for which the upregulation was sustained until day 3 (Figure 5). *IL-10*, an anti-inflammatory cytokine, showed a unique gene expression pattern with a later activation on day 3 by Muc gel, followed by a decrease on day 7. Strikingly, *IL-10* was significantly upregulated by tMuc gel on day 1. The expression of *CD64* in THP-1-M0 cultured on tMuc gel was significantly higher than Muc gel on day 1, however, there was no significant difference compared to TCP. *MRC1* downregulation was less dependent on sialic acid since it was expressed in cells cultured both on Muc gel and tMuc gels. *Tgm2* (M2 marker) did not change compared to TCP control on day 1 but was downregulated on day 7. The expression of *Tgm2* was downregulated by tMuc gels on day 3 when compared to Muc gels. For nearly all markers, THP-1-M0 cultured on tMuc gels led to little or no activation on days 1 and 3, in contrast with the strong transient activation observed in THP-1-M0 cultured on Muc gels.

We confirmed the gene expression by measuring the expression of four intracellular cytokines at the protein level by FACS. As shown in Figure 6, for *IL1Ra*, *IL-1B*, and *CXCL8* in THP-1-M0, the results were consistent with gene expression, with a significant upregulation in THP-1-M0 cultured on Muc gels when compared to TCP on day 1. Reduction in sialic acid content also led to an inhibition of the transient activation of the macrophages. There were also some discrepancies with the gene expression data. *IL-1B* was downregulated on day 3 but maintained at significantly higher level than on tMuc gels. *IL10* protein expression was significantly upregulated by Muc gels on days 1 and 3, which does not agree with the low gene

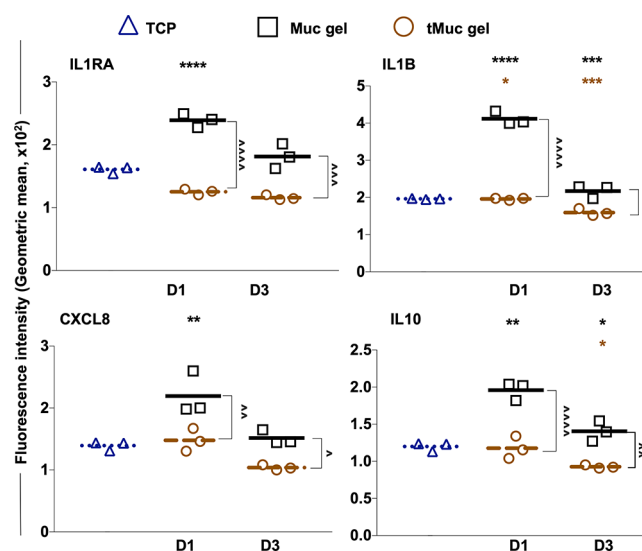


Figure 6. Intracellular cytokine expressions at the protein level in THP-1-derived macrophages type 0 (THP-1-M0) after being cultured on tissue culture polystyrene (TCP), Muc gels, and sialidase-treated Muc gels (tMuc gel) on D1 and D3, analyzed by FACS. The data denote the geometric mean of fluorescence intensity from three independent experiments. Statistics were obtained by one-way ANOVA test by Prism 8.0. Black *, brown *, and black ^ indicate the comparison between Muc gels vs TCP, tMuc gels vs TCP, and Muc gel vs tMuc gel, respectively. *, **, ***, and **** indicate *p* values of <0.05, 0.01, 0.0005, and 0.0001, respectively.

expression level for *IL10* in THP-1-M0 culture on Muc gels on day 1.

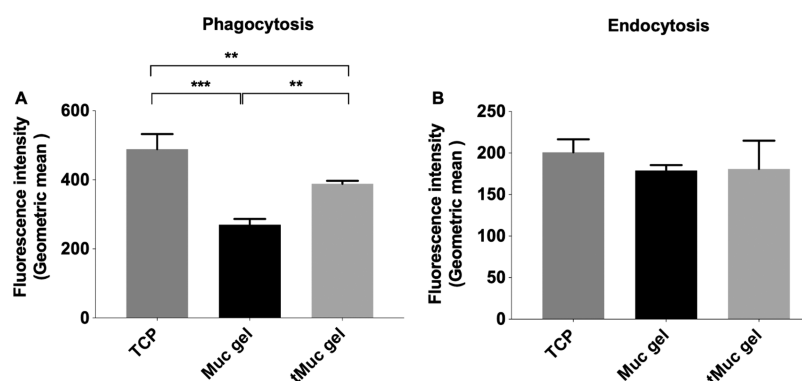


Figure 7. Phagocytosis and endocytosis of THP-1-M0 cells cultured on tissue culture polystyrene (TCP), Muc gels, and sialidase-treated Muc gels (tMuc gel) for 1 day and analyzed by FACS. Cells were treated with pHrodo green *E. coli* bioparticles to measure phagocytosis (A) and fluorescein-labeled dextran (10 kDa, Sigma-Aldrich) to measure endocytosis (B). Data reflect three independent experiments. Statistics were obtained via one-way ANOVA test among cells cultured on three different surfaces. *, **, ***, and **** indicate *p* values of <0.05, 0.01, 0.0005, and 0.0001, respectively.

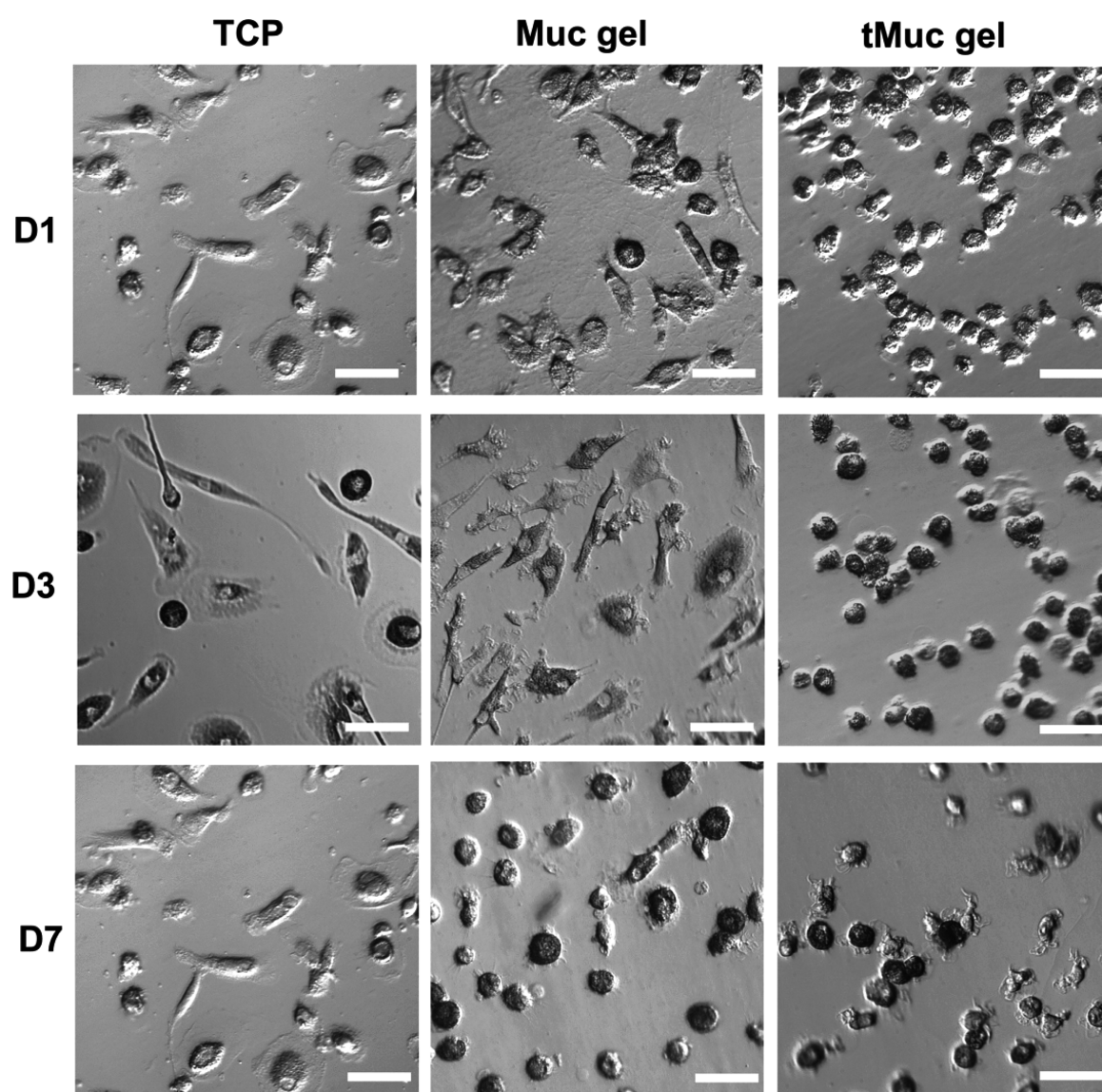


Figure 8. Representative phase-contrast images of hPBMC-M0 cultured on tissue culture polystyrene (TCP), Muc gel, and tMuc gels on D1, D3, and D7. Scale bar = 50 μm .

Decrease of Phagocytic Ability of THP-1-M0 When Cultured on Muc Gels but No Change in Their

Endocytotic Ability. In addition to major changes in the expression of cell markers and cytokines, the polarization of

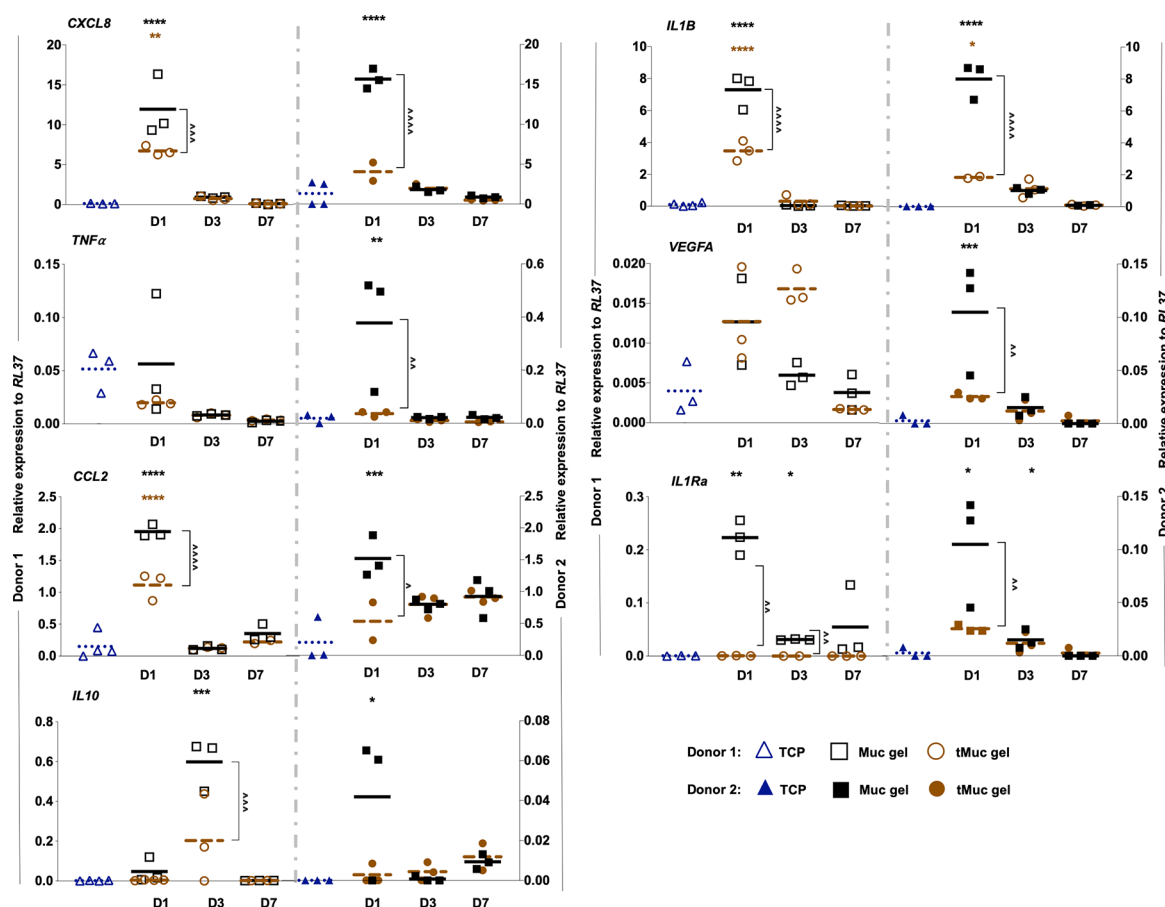


Figure 9. Gene expression in human peripheral blood monocytes-derived macrophages type 0 (hPBMC-M0) after being cultured on tissue culture polystyrene (TCP), Muc gels, and sialidase-treated Muc gels (tMuc gel) on D1, D3, and D7. The data denote the mean of relative gene expression to RPL-37 obtained from three independent repeats with duplicates. Donors 1 and 2 are hollow and filled shapes, respectively. Statistics were obtained by one-way ANOVA test by Prism 8.0. Black *, brown *, and black ^ indicate the comparison between Muc gels vs TCP, tMuc gels vs TCP, and Muc gel vs tMuc gel, respectively. *, **, ***, and **** indicate p values of <0.05, 0.01, 0.0005, and 0.0001, respectively.

macrophages also results in functional differences. In particular, the tendency of macrophages to uptake foreign objects by either endocytosis or phagocytosis has been associated with macrophages phenotypes *in vitro*.²² We thus investigate the phagocytosis and endocytosis capacities of THP-1-M0 after culturing them on TCP, Muc gel, or tMuc gel for 1 day. We show the Muc gel dampened the phagocytic activity of M0 but did not change their endocytic activity (Figure 7). Cells cultured on tMuc gel showed a similar trend but with a less pronounced decrease in the phagocytic activity.

Macrophages Type 0 Derived from Human Peripheral Blood Monocytes (hPBMC-M0) are Also Activated by Muc Gels in a Sialic Acid-Dependent Manner. Although the protocol used to obtain macrophages from THP-1 monocytes has been optimized to generate macrophages best resembling primary monocyte-derived macrophages, there persist differences in how they respond to stimuli.³³ We thus studied the response of human peripheral blood monocytes derived macrophages type 0 (hPBMS-M0) when cultured on Muc gels to increase the further validation of the biological relevance of the results presented above. We sorted human monocytes (CD3⁺CD19⁺CD14⁺) by FACS based on cell surface markers (Figure S8). The monocyte–macrophage differentiation was performed by incubation with macrophage colony-stimulating factor (M-CSF). The differentiated macrophages became adherent and expressed macrophage markers

(Figure S9). hPBMC-M0 cells were cultured on three different surfaces TCP, Muc gels, and tMuc gels over a period of 7 days. hPBMC-M0 were elongated on TCP on days 1, 3, and 7, spindle-shaped on Muc gels, and round with dendrites on tMuc gels (Figure 8). The cell-cultured on Muc gels and tMuc gels could be detached by pipetting, indicating a rather weak adhesion.

We investigated the gene expression of seven cytokines in hPBMC-M0 cells on days 1, 3, and 7. Both pro-inflammatory cytokines (CXCL8, IL1B, and CCL2) and anti-inflammatory (IL1Ra and IL-10) cytokines were significantly upregulated in cells from donor 1 and donor 2 cultured on Muc gels on day 1 and then downregulated on days 3 and 7 (Figure 9). However, TNF α and VEGFA upregulations on day 1 by Muc gels were only observed for donor 2. The partial removal of sialic acids in tMuc gels dampened the transient upregulation of most cytokines down to the levels in cells cultured on TCP. Exceptions were for VEGFA and TNF α for donor 1 and IL10 for donors 1 and 2 for which there was not a statistically significant difference between Muc and tMuc gels. It is difficult to explain or predict the exact functional implications of the differences observed between the two donors. However, these differences reflect the impact of the cell genetic background and phenotypal state of the immune cells in their response to materials and suggest that the immune-modulating capacity of Muc gels could somewhat vary between individuals.

DISCUSSION

The development and characterization of the Muc gel described herein serve two fundamental purposes. First, because Muc gels mimic the gel-phase presentation of secreted mucins in mucus, or membrane-bound mucins as part of the cell glycocalyx, they are interesting models to further investigate the bioactivity of mucin glycoprotein toward immune cells.¹⁵ The assembly of mucins into hydrogels can possibly change the local concentrations of ligands, affect the internalization of receptors, and engage other receptors interacting with the material such as integrins that can cross-talk with mucin-binding receptors. These phenomena are well established for certain growth factors; for instance, tethered EGF³⁴ or BMP³⁵ show different responses than when presented in solution. Second, mucin biomaterials appear as promising immune-modulating systems for tissue engineering and regenerative medicine. Other extracellular matrix molecules (ECMs) are appearing as promising building blocks of immune-modulating scaffolds and biointerfaces.³⁶ For instance, hyaluronic acid (HA) was shown to participate in the immune-dampening effect of the tumor microenvironment,³⁷ and mediated activation of $\alpha v \beta 3$ integrins leading to a anti-inflammatory M2 macrophage phenotype.³⁸ And fibrillar rat type I collagen 3D scaffold affects macrophage polarization toward M2 in an integrin-dependent fashion.³⁹

The bovine submaxillary mucins (BSMs) used herein contain about 50% sialyl Tn and 10% Tn antigens. The sialic acid residues, composed of ~70% Neu5Ac and ~30% Neu5Gc can make up to 30% of the molecule's mass.^{40,41} A number of non-sialylated N-glycans are also present on the BSM.⁴² Sialic acids are of particular interest in this study since they play important roles in immunity. Physically, owing to their localization at the tip of the glycosylation and their negative charge, sialic acid mediate cell–cell interactions and mask antigens. Biologically, by acting as a ligand to several sialic acid-binding receptors on immune cells, sialic acid regulates the activation of the complement, leukocyte trafficking, and the immunoactivity of dendritic cells, neutrophils, B cells, T cells, and macrophages.^{43–45} An important class of sialic acid receptors are sialic acid-binding immunoglobulin-like lectins (siglec). *In vitro* cultured human monocytes-derived macrophages express siglec-1, siglec-3, siglec-7, siglec-9, and siglec-10.⁴⁶ The THP-1-M0 induced by PMA used in this study express siglec-1, siglec-3, siglec-5, siglec-6, siglec-8, and siglec-10.^{47,48} Out of these siglecs, at least siglec-1, siglec-3, siglec-8,⁴⁹ siglec-9,^{40,50} and siglec-15,⁵¹ were shown to bind either strongly or moderately the sialyl Tn antigen presented in BSM. These binding events will lead to both activation or dampening of the immune response. For instance, in dendritic cells, neutrophils and macrophages, siglec-2, siglec-3, and siglec-5 to -11 regulate cytokine expression by inhibiting the toll-like receptor signaling pathway when bound to sialic acid residues of mucins^{40,52,53} and other sialic acid-bearing ligands.⁵⁴ Beatson *et al.* reported mucin MUC1 expressed on cancer cells, which is decorated by multiple short, sialylated O-linked glycans, engages siglec-9 on myeloid cells, and “educates” them toward pro-tumoral phenotype, contributing to a tumor immunosuppressive microenvironment.⁵⁵ In contrast, activated siglec-14, -15, and -16 can associate with DAP12, resulting in the activation of MAPK and AKT pathways, thereby stimulating the pro-inflammatory response.⁵⁶ In addition, in antigen-presenting cells, siglec-1 is involved in the binding and internalization of sialic acid-

containing antigens before their surface presentation to dendritic and T cells.⁴⁶

To investigate the relatively short-term immune-modulatory effect of Muc gels, we cultured both THP-1-M0 and hPBMC-M0 macrophages for 7 days at the gel surfaces. We decreased the sialic acid content of the Muc gels (tMuc gels) to investigate the role of sialic acid in the response of macrophages. The similar mechanical properties and levels of endotoxin and DNA impurities between Muc and tMuc gels (Figure S10) ensure that the effects observed on macrophages are solely due to the removal of sialic acid. Indeed the mechanical properties of the cellular substrate can affect a host of cell processes⁵⁷ and impurities in the material alone can activate macrophages.⁵⁸ On the basis of previous reports of the impact of substrate stiffness on macrophage modulation, the slightly smaller average modulus for tMuc gels compared to Muc gel is not likely to be sufficient to impact macrophage phenotype to the extent we observed.²⁵ We show sialic acid residues on mucins are not crucial for the formation of the cross-linking knots of Muc gels. We hypothesize that this is because the EDC/NHS chemistry applied to graft the Tz and Nb functionalities mainly targets carboxylic groups on the mucin–protein backbone.²¹ The localization of Tz/Nb functionalities on the protein backbone is also supported by the absence of Tz and Nb ¹H NMR peaks in the glycan fraction after their removal from mucins by β -elimination, while strong Tz and Nb ¹H NMR peaks were detected from the protein fraction (Figure S1). However, since β -elimination does not remove all mucin glycans and sialic acid residues, it is still possible that the absence of Tz and Nb in the glycan fraction is explained by their exclusive localization on glycans resistant to β -elimination.

After implantation, neutrophils are one of the first immune cells recruited during the acute inflammatory response.^{59,60} Monocytes follow, and can differentiate into, macrophages in response to various environmental cues, including growth factors such as macrophage colony-stimulating factor and IL1B. Macrophages then play an important role in the immune response to implanted biomaterials. We thus focused on characterizing the interactions of nonpolarized macrophages, both THP-1-M0 and hPBMC-M0, with the surface of Muc and tMuc gels. The Muc gels and tMuc are non-cytotoxic and support the survival of cells seeded on (Figure S6) or in²¹ the hydrogels for 7 days. Both THP-1-M0 and hPBMC-M0 poorly adhered to the surface of Muc and tMuc gels. And although hPBMC-M0 spread and did not form clusters, pipetting alone was sufficient to detach them from the surface. This did not come as a surprise, as the materials carry similarities with other poorly cell adherent materials such as alginate⁶¹ and hyaluronic acid⁶² that are also hydrated and do not carry any known binding ligands to integrins. This is also in agreement with previous reports of mucin coatings preventing cell adhesion.⁶³

Then, we aimed to characterize the possible polarization resulting from contact with the Muc gels. The primary hallmark is a general activation of cytokine gene expression and protein production in THP-1-M0 and hPBMC-M0 when in contact with the Muc gels, followed by a reduction on day 3 and back to baseline on day 7. A few exceptions to this general trend were observed. Compared to hPBMC-M0, THP-1-M0 macrophage expression of *MRC1* was not upregulated and *CXCL8*, *VEGFA*, and *IL1RN* differed in their kinetics, with a sustained upregulation on day 3 by Muc gel. The M1 surface markers CD64, a transmembrane glycoprotein involving in antibody-dependent cellular cytotoxicity,⁶⁴ was significantly dampened in

THP-1-M0 by Muc gels on day 1 and by tMuc gels on day 3. There were some inconsistencies for *IL10* expression at the gene and protein level and between THP-1-M0 and PBMC-M0. The delayed *IL10* upregulation by Muc gels was only observed in THP-1-M0 and at the gene level. The protein levels in THP-1-M0 and gene expression in hPBMC-M0 were more consistent with an increased expression on day 1. The sustained protein levels of *IL10* in THP-1-M0 on Muc gels on day 3 could be partially explained by the difference in the lifetimes of mRNA and protein. Overall, it is likely that the combined signaling of several cell surface receptors followed by regulatory mechanisms that result in this complex cytokine expression pattern.

In addition to the expression of markers, THP-1-M0 on Muc gels significantly affected their phagocytosis (Figure 7A) but not their endocytic activity (Figure 7B). This may be explained by the downregulation of *MRC1* by Muc gels and tMuc gels. *MRC1* acts as a phagocytic receptor *via* binding to high-mannose structures presented on bacteria, fungi, and other pathogens.⁶⁵ Overexpression in human macrophages of the *MUC1* mucin, which contains glycosylation similar to BSM also led to the decrease of their phagocytic activity.⁶⁶ Interestingly, M1 macrophages polarized by IFN γ or LPS and IFN γ were shown to decrease their phagocytic ability compared to M0,²² which is consistent with our results. However, there is not sufficient evidence to conclude that contact between M0 macrophages and a Muc gel would result in an M1 phenotype. Thus, neither the expression of cytokines, cell marker, or the functional signature of macrophages suggests that M0 macrophages polarize toward M1 or M2 after contact with Muc or tMuc gels. The activation of macrophages described herein and in previous work²¹ support the existence of a continuum of macrophage phenotypes between M1 and M2,⁶⁷ especially *in vivo*.⁶⁸ Indeed, the details in how macrophages are activated depend on numerous factors such as the combination of biochemical signals, cell type, and kinetics. Complex environments encountered *in vivo*, or contact with complex materials such as Muc gels, would impact several of these factors.

To test the role of sialic acid in the immune-modulating activities observed, we treated the Muc gels with sialidase. Although sialic acids were not completely absent in tMuc gels, a relative decrease compared to Muc gel still led to drastic changes in the macrophages' response to the material. This suggests the important role of sialic acid receptors such as siglecs on macrophages that regulate their activities, without excluding the role of other sugars. Indeed, tMuc gels with low sialic acid contents activated *IL10* on day 1 and downregulated *CD64*, *CXCL10*, and *CCL2* on days 3 and 7; *MRC1* on days 1, 3, and 7 in THP-1-M0; *CXCL8*, *CCL2* in donor 1, and *ILB* in donors 1 and 2 on day 1 (Figures 5 and 9, brown *) compared to unmodified Muc gels.³⁸ When removing the sialic acid, the sialyl Tn antigens are converted to Tn antigens. This, in turn, can become a binding partner for a number of receptors, including the macrophage galactose type C-type lectin.⁶⁹ The bioactivities of the Tn antigens are also many⁷⁰ and will certainly add to the overall effect of Muc gels on macrophages seen in this study.

CONCLUSION

In this study, we characterized the short-term response of macrophages to Muc gels and investigated the role of sialic acid in the bioactivity of the material. We were able to modulate the glyco-composition of mucin hydrogels without altering their bulk rheological properties and nanomechanical surface properties. We show Muc gels transiently activate macrophages in a

sialic acid-dependent manner. Macrophages exposed to Muc gels could not be classified as M1 or M2, but showed broad expression of cytokines on day 1 followed by a decrease on days 3 and 7, with only a few exceptions. How these macrophage activation patterns translate into the broader immune reaction to implantation is unclear. In part because macrophages expression patterns and biomaterial implant outcomes are not well correlated and in another part because of the absence of many other immune components in our *in vitro* system. However, the low cytokine expression could be correlated with the low cytokine expression levels found 14 and 21 days after implantation of Muc gels in the intraperitoneal space of mice, which could be linked with high expression levels of cytokine inhibitor proteins.²¹ This study also demonstrates that the glyco-modulation of cross-linkable mucin building blocks serves as a valuable tool to study the bioactivities of mucin materials. Such an approach could be expanded to establish a series of mucin hydrogel variants to study the interplay between glycan composition and cell response. For instance, this study highlights the importance of sialic acid in immune-modulating properties of Muc gels and suggests sialic acid immobilized on a backbone polymer could be a good candidate for artificial mucins recapitulating some of their intrinsic immune-modulating properties.⁷¹

MATERIALS AND METHODS

Materials. Tetrazine amine (Tz) and norbornene amine (Nb) were purchased from Bioconjugate Technology Co. and TCI EUROPE N.V., respectively. All chemicals were obtained from Sigma-Aldrich including bovine submaxillary mucins (BSM). Given that BSM is a natural material that can experience batch to batch variation, we have conducted these experiments with two batches of BSM (SLBS0651 V and SLBL5233 V). No difference in the effects on macrophages was observed. Cell culture medium and PCR related reagents were purchased from ThermoFisher Scientific. RNA extraction micro- or minikits were purchased from Qiagen. Human monocytes (THP-1) were purchased from ATCC, and human peripheral blood was purchased from a blood bank at the Karolinska Institute Hospital.

Synthesis of Mucin Tz and Nb Derivatives. We introduced Tz and Nb cross-linking functionalities onto mucins (Muc-Tz and Muc-Nb) as described before.²¹ In brief, mucin was predissolved in MES buffer (0.1 M MES, 0.3 M NaCl, and pH 6.5) at a concentration of 10 mg/mL. 1-Ethyl-3-(3-dimethylaminopropyl)carbodiimide (EDC; 4 mmol/(g of dry mucin)) and *N*-hydroxysuccinimide (NHS; 4 mmol/(g of dry mucin)) were then added and stirred for 15 min at room temperature. To the mixture, tetrazine (1 mmol/(g of mucin)) and norbornene (2 mmol/(g of mucin)) were added individually. The reaction mixtures were stirred at 4 °C overnight. After reaction, the reaction mixtures were dialyzed in 100 kDa cutoff-dialysis tubing for 2 days against 300 mM NaCl followed by dialysis against Milli-Q H₂O for 1 day. Samples were freeze-dried and stored in −20 °C. Specifically, samples used for cell culture were filtered by a syringe filter (0.45 μ m) and then transferred into tissue culture flat tubes (screw cap with filter, 0.2 μ m) for lyophilization to keep them sterile.

Glycan Modification and Characterization. The sialic acid removal assay was conducted by using neuraminidase immobilized on slurries (GlycoCleave Neuraminidase kit, GALAB technologies). Briefly, the gelling components of Muc-Tz and Muc-Nb were dissolved separately in a sodium acetate buffer (0.05 mM sodium acetate, 1 mM CaCl₂, pH 5.5) at a concentration of 25 mg/mL. The solution was then mixed with 1 mL of neuraminidase slurry and incubated overnight at 37 °C at 30 rpm. To separate the neuraminidase slurry and the enzyme-treated mucin derivatives, the mixture was passed through a 10 μ m filter. The slurry was washed twice with an acetate buffer. After that, the flow-through was loaded into an Amicon Ultra-30K filter and then centrifuged at 4000g for 30 min to separate the enzyme-treated mucin and other small molecules. Next, 15 mL of MQ H₂O was added to the

mucin fraction and then centrifuged at 4000g, 30 min three times to desalt the solution. Sterilization was performed by a syringe filter (0.45 μm); then the samples were loaded into tissue culture tubes equipped with screw caps with filter (0.2 μm). Samples were freeze-dried and stored at -20°C .

The removal efficiency of sialic acid was investigated by anion exchange chromatography based assays. In brief, neuraminidase-treated mucins were further treated by sulfuric acid to cleave all of the glycans. Nontreated mucins were also treated by sulfuric acid and were used for quantification of the sialic acid content of mucin.

Sialic acid quantification was conducted by using the anion exchange chromatography based assay as described above.

Rheological Characterization of Muc Gels. Rheological measurements were performed using a research-grade shear rheometer (MCR302, Anton Paar) equipped with a plate–plate measuring geometry (measuring head, PP25; Anton Paar, Graz, Austria). The gap between the measuring head and the bottom plate (P-PTD200/Air, Anton Paar) was set to $d = 150\ \mu\text{m}$ for all measurements. Immediately before a measurement, the two components (Muc-Tz and Muc-Nb) of either the Muc gel or the tMuc gel were diluted in the particular buffer to a concentration of 25 mg/mL each. As a buffer solution, either PBS (pH = 7.4) or a mixture of RPMI 1640 (R8758, Sigma-Aldrich, St. Louis, MO, USA) containing 10% FBS (F9665, Sigma-Aldrich) and 1% penicillin and streptomycin (P4333, Sigma-Aldrich) was used. The two components were thoroughly mixed and centrifuged to remove bubbles before 100 μL of the sample was pipetted onto the rheometer plate. First, gel formation was analyzed for a total time span of $t = 100\ \text{min}$. Both the storage (G') and loss modulus (G'') were determined by a torque-controlled ($M = 5\ \text{mN}$) oscillatory ($f = 1\ \text{Hz}$) measurement. Afterward, a strain-controlled frequency sweep (from $f_{\text{start}} = 10\ \text{Hz}$ to $f_{\text{end}} = 0.01\ \text{Hz}$) was performed to determine the frequency-dependent viscoelasticity of the cross-linked sample. For this frequency sweep, a constant strain was used, which was chosen as the average of the five last values determined in the torque-controlled gelation measurement.

Surface Nanomechanical Properties of Gels by Atomic Force Microscopy. Silicon wafers ($22 \times 22\ \text{mm}^2$) were cleaned using a 2% Deconex solution (Borer Chemie AG, Switzerland) in a sonicator for 15 min, then rinsed with Milli-Q water and ethanol sequentially, and dried using a filtered nitrogen jet. The gelling components for Muc gels and tMuc gels were premixed and deposited on substrates separately and incubated for 1 h in a humidified chamber to allow proper gelation. The nanomechanical measurements were conducted in force volume mapping mode using a JPK NanoWizard 3 atomic force microscope (JPK Instruments AG, Berlin, Germany). Before the measurements, a drop of PBS is loaded onto the gel to have an aqueous phase. The EBD biosphere B100-CONT (Nanotools) probe of a well-calibrated and measured sphere tip outer radius of 100 nm and a measured spring constant of 0.26 N/m was used for nanoindentation measurements. The acquired force curves were analyzed using standard JPK data processing software (JPK, version 6.1.86). The Derjaguin–Muller–Toporov (DMT) model was fitted to determine the elastic modulus on approaching and retracting force curves following a previous publication.²⁸ The force volume maps were measured on an area of $2 \times 2\ \mu\text{m}^2$ with 8 by 8 data points. The applied normal force was 0.3 nN, and the acquisition speed was 4 $\mu\text{m/s}$. Three different areas of $2 \times 2\ \mu\text{m}^2$ were measured in order to evaluate the average nanomechanical parameters. We observed differences in the nanomechanical surface properties between the approach and retract mapping regimes for both Muc gels (Figure 3A,B) and tMuc gels (Figure 3A,B). These are possibly due to the different contributions in each regime, with combined elastic and viscous contributions in the approach maps, and a predominant elastic contribution in the retraction maps. This also indicates the importance of analyzing both approaching and retraction regimes in AFM force volume mapping for soft materials, the surface dynamics of which should be taken into account and a complicated tip–surface interaction occurs in the measurements.^{28,72} Moreover, commonly applied contact mechanics models such as Hertz and/or the DMT are limited for studying soft gels due to the substantial viscous contribution from those soft gels. We thus also evaluated surface stiffness parameters, which do not require any contact mechanics model

fitting and can be more suitable for the direct comparison of the nanomechanical surface property of Muc gels and tMuc gels using the same AFM probe.

THP-1 Cell Cultivation and Differentiation. Human monocytes THP-1 were purchased from ATCC and cultured in RPMI-1640 medium supplemented with 10% FBS, and penicillin/streptomycin (100 U/mL). Cells were split at the ratio of 1/5 when the cell density reached $1 \times 10^6\ \text{cells/mL}$. To differentiate cells into macrophage type 0 (M0), the THP-1 cells were cultured in the culture medium used above and supplemented with 150 nM phorbol 12-myristate 13-acetate (PMA, Sigma-Aldrich) for 72 h, followed by 24 h incubation in a complete cell culture medium without PMA. To confirm the differentiation of THP-1, the cell morphological change was examined under bright field microscope and macrophage markers CD36 (2.5 μg per $1 \times 10^6\ \text{cells}$ in 100 μL ; Cat. No. 108418, BioLegend) and CD71 (2.5 μg per $1 \times 10^6\ \text{cells}$ in 100 μL ; Cat. No. 108418, BioLegend) were evaluated by FACS.

Human Monocytes Isolated from Peripheral Blood and Differentiation. Human monocytes were isolated from human peripheral blood from 2 donors purchased from the Blood Bank at Karolinska Sjukhuset. Mononuclear cells were acquired by using Ficoll-Paque PREMIUM density gradient media (GE Healthcare Life Science) according to the instruction. Briefly, blood was diluted with PBS at a ratio of 4/5, which then was carefully layered onto the Ficoll-Paque media at the ratio of 4/5. To obtain the mononuclear cell, the samples were then centrifuged at 700g for 40 min with acceleration and deceleration speed level at 4. The serum was sterilized by using 0.45 μm filters and stored at 4°C for further usage. The mononuclear cells were washed in PBS and centrifuged for 10 min at 700g to remove the Ficoll media. The cells were cleaned through a 70 μm cell strainer (Corning) to get rid of clumps and then counted using a Bürker chamber. Monocytes were enriched by using a monocytes enrichment kit (BD Biosciences) according to the manufacture instructions. The cells were resuspended in an IMAG buffer solution and incubated with the monocyte enrichment cocktail and CD41 antibodies at a concentration of 5 μL per $1 \times 10^6\ \text{cells}$ for 15 min. The nonconjugated antibodies were washed away by IMAG buffer, the cell pellet was then resuspended in IMag streptavidin Particles Plus-DM at the concentration of 5 μL per $1 \times 10^6\ \text{cells}$ for 15 min. The enriched monocytes fraction was negatively selected and further sorted by FACS. Briefly, the monocytes were incubated for 10 min at room temperature with human BD Fc-block (2.5 μg per $1 \times 10^6\ \text{cells}$ in 100 μL , Cat. No. 564220, BD Biosciences). The cells were further incubated with the following antibody cocktail for 30 min at 4°C : APC-H7 Mouse Anti-Human CD3 Clone M-A712 (2.5 μg per $1 \times 10^6\ \text{cells}$ in 100 μL , Biolegends), PE Mouse Anti-Human CD14 Clone M5E2 (2.5 μg per $1 \times 10^6\ \text{cells}$ in 100 μL , Biolegends), and BB515 Mouse Anti-Human CD19 Clone HIB19 (2.5 μg per $1 \times 10^6\ \text{cells}$ in 100 μL , Biolegends). Cells were washed with 5 mL of PBS and then resuspended in 5 mL of PBS containing 20% serum. The cells within the gate of CD3-CD19-CD14+ were then sorted using FACS.

To differentiate the monocytes into M0, monocytes were cultured in RPMI-1640 medium supplemented with 20% endogenous serum, penicillin/streptomycin (100 U/mL), and macrophage colony-stimulating factor (M-CSF, Gibco, 1 μg per 5 mL of medium, Cat. No. PHC9501, Gibco) in a T-25 culture flask for 5 days.

Gene Expression Analysis by Real-Time PCR. The total RNA of cells was extracted by using either Qiagen RNeasy minikit or Qiagen RNeasy microkit depending on the cell numbers obtained. The extracted mRNA was diluted to a concentration of 0.67 ng/ μL and synthesized into cDNA using Superscript III polymerase (Invitrogen). Real-time PCR was then performed to analyze the gene expression by using a TaqMan Gene Expression Master Mix (Thermo Fisher Scientific) together with TaqMan probes. See the TaqMan probes in Supporting Information Table S1. The RT-PCR were carried out in a CFX96 Touch Real-Time PCR Detection System (Bio-Rad) with the following cycling conditions: 50°C for 2 min, 95°C for 10 min, 95°C for 15 s, 60°C for 1 min, and then go to step 3 for 50 cycles. RPL37 was used for THP-1-M0, while ACTB was used as housekeeping gene for primary monocytes derived macrophages (PBMC-M0).

Intracellular Cytokine Expression by FACS. THP-1-M0 cells cultured on TCP, Muc gels, and tMuc gels were incubated with brefeldin A buffer (diluted to 1× with complete cell culture medium, Cat. No. 420601, Biolegend) for 5 h. Cells were then harvested, washed with a washing buffer (PBS containing 0.5% bovine serum albumin (BSA) and 0.1% sodium azide) twice, and then resuspended in a FACS permeabilizing solution (Cat. No. 347692, BD Bioscience) for 10 min at room temperature. After permeabilization, cells were washed with 1 mL of a washing buffer and centrifuged at 500 g for 5 min. Cell pellets were then incubated with 500 μ L of 1% paraformaldehyde at room temperature and then washed twice with a washing buffer. Cells were then incubated with an antibody cocktail for 30 min on ice, containing anti-IL1RN (10 μ L per 1×10^6 cells in 100 μ L, Cat. No. 340525, BD Bioscience), anti-IL1B (5 μ L per 1×10^6 cells in 100 μ L, Cat. No. 340515, BD Bioscience, recognizing the processed and secreted form of IL-1B), anti-IL10 (5 μ L per 1×10^6 cells in 100 μ L, Cat. No. 562400, BD Bioscience), and anti-IL8 (5 μ L per 1×10^6 cells in 100 μ L, Cat. No. 563310, BD Bioscience). Cells were then washed and resuspended in the washing buffer before being subjected to FACS analysis.

Phagocytosis and Endocytosis. pHrodo green *Escherichia coli* (*E. coli*) bioparticles (LifeTech) and fluorescein labeled dextran (10 kDa, Sigma-Aldrich) were used to investigate the phagocytosis and endocytosis function of THP-1-derived M0. Briefly, cells were seeded on TCP, Muc gels, and tMuc gels. After 1 day, cells were then incubated with either dextran or *E. coli* bioparticles (5 μ g/mL) for 60 min at 37 °C. Cells without treatment served as negative control. The internalization of the particles was then quantitatively measured by the geometric mean of fluorescence intensities (GMFI) using flow cytometry.

Statistical Analysis. Data are shown as a means of three independent experiments. The significance was analyzed via non-parametric one-way ANOVA test using GraphPad Prism 8.0; *, **, ***, and **** indicate *p* values of <0.05, 0.01, 0.0005, and 0.0001, respectively.

■ ASSOCIATED CONTENT

Supporting Information

The Supporting Information is available free of charge at <https://pubs.acs.org/doi/10.1021/acsami.0c03645>.

Methods and other details including ¹H-NMR detection after β -elimination, rheological characterization of Muc gels, approach/retract mechanical mappings, expression of THP-1-M0 macrophage markers, gene expressions, representative FACS profiles, macrophage markers' expression, TaqMan probes used for gene expression assays; abbreviations of cytokines (PDF)

■ AUTHOR INFORMATION

Corresponding Author

Thomas Crouzier – Division of Glycoscience, Department of Chemistry, School of Engineering Sciences in Chemistry, Biotechnology and Health, KTH, Royal Institute of Technology, 106 91 Stockholm, Sweden; orcid.org/0000-0002-1981-3736; Email: crouzier@kth.se

Authors

Hongji Yan – Division of Glycoscience, Department of Chemistry, School of Engineering Sciences in Chemistry, Biotechnology and Health, KTH, Royal Institute of Technology, 106 91 Stockholm, Sweden

Morgan Hjorth – Division of Glycoscience, Department of Chemistry, School of Engineering Sciences in Chemistry, Biotechnology and Health, KTH, Royal Institute of Technology, 106 91 Stockholm, Sweden

Benjamin Winkeljann – Department of Mechanical Engineering and Munich School of Bioengineering, Technical University of Munich, 85748 Garching, Germany

Illia Dobryden – Division of Surface and Corrosion Science, Department of Chemistry, School of Engineering Sciences in Chemistry, Biotechnology and Health, KTH Royal Institute of Technology, 10044 Stockholm, Sweden; orcid.org/0000-0001-6877-9282

Oliver Lieleg – Department of Mechanical Engineering and Munich School of Bioengineering, Technical University of Munich, 85748 Garching, Germany; orcid.org/0000-0002-6874-7456

Complete contact information is available at: <https://pubs.acs.org/doi/10.1021/acsami.0c03645>

Notes

The authors declare no competing financial interest.

■ ACKNOWLEDGMENTS

T.C. acknowledges financial support from the Swedish Foundation for Strategic Research (Grant No. FFL15-0072), FORMAS (Grant No. 2015-1316), and the Swedish Research Council (Grant No. 2014-6203). O.L. acknowledges financial support from the Deutsche Forschungsgemeinschaft (DFG) through Project B11 in the framework of SFB863. We acknowledge Francisco Javier Vilaplana Domingo from KTH for assistance with sialic acid quantification.

■ REFERENCES

- (1) Zhao, Y.; Yan, H.; Qiao, S.; Zhang, L.; Wang, T.; Meng, Q.; Chen, X.; Lin, F. H.; Guo, K.; Li, C. F.; Tian, W. M. Hydrogels Bearing Bioengineered Mimetic Embryonic Microenvironments for Tumor Reversion. *J. Mater. Chem. B* **2016**, 4 (37), 6183–6191.
- (2) Zheng, H. X.; Liu, S. S.; Tian, W. M.; Yan, H. J.; Zhang, Y.; Li, Y. A Three-Dimensional in Vitro Culture Model for Primary Neonatal Rat Ventricular Myocytes. *Curr. Appl. Phys.* **2012**, 12 (3), 826–833.
- (3) Zhao, Y. F.; Qiao, S. P.; Shi, S. L.; Yao, L. F.; Hou, X. L.; Li, C. F.; Lin, F. H.; Guo, K.; Acharya, A.; Chen, X. B.; Nie, Y.; Tian, W. M. Modulating Three-Dimensional Microenvironment with Hyaluronan of Different Molecular Weights Alters Breast Cancer Cell Invasion Behavior. *ACS Appl. Mater. Interfaces* **2017**, 9 (11), 9327–9338.
- (4) Duffy, C. V.; David, L.; Crouzier, T. Covalently-Crosslinked Mucin Biopolymer Hydrogels for Sustained Drug Delivery. *Acta Biomater.* **2015**, 20, 51–59.
- (5) Yan, H. J.; Casalini, T.; Hulsart-Billström, G.; Wang, S.; Oommen, O. P.; Salvalaglio, M.; Larsson, S.; Hilborn, J.; Varghese, O. P. Synthetic Design of Growth Factor Sequestering Extracellular Matrix Mimetic Hydrogel for Promoting in Vivo Bone Formation. *Biomaterials* **2018**, 161, 190–202.
- (6) Bartneck, M.; Heffels, K. H.; Pan, Y.; Bovi, M.; Zwadlo-Klarwasser, G.; Groll, J. Inducing Healing-like Human Primary Macrophage Phenotypes by 3D Hydrogel Coated Nanofibres. *Biomaterials* **2012**, 33 (16), 4136–4146.
- (7) Sridharan, R.; Cameron, A. R.; Kelly, D. J.; Kearney, C. J.; O'Brien, F. J. Biomaterial Based Modulation of Macrophage Polarization: A Review and Suggested Design Principles. *Mater. Today* **2015**, 18 (6), 313–325.
- (8) Chen, Z.; Klein, T.; Murray, R. Z.; Crawford, R.; Chang, J.; Wu, C.; Xiao, Y. Osteoimmunomodulation for the Development of Advanced Bone Biomaterials. *Mater. Today* **2016**, 19 (6), 304–321.
- (9) Shields, C. W., IV; Wang, L. L.-W.; Evans, M. A.; Mitragotri, S. Materials for Immunotherapy. *Adv. Mater.* **2020**, 32, 1901633.
- (10) Ali, O. A.; Tayalia, P.; Shvartsman, D.; Lewin, S.; Mooney, D. J. Inflammatory Cytokines Presented from Polymer Matrices Differentially Generate and Activate DCs in Situ. *Adv. Funct. Mater.* **2013**, 23 (36), 4621–4628.
- (11) Petrou, G.; Crouzier, T. Mucins as Multifunctional Building Blocks of Biomaterials. *Biomater. Sci.* **2018**, 6 (9), 2282–2297.

- (12) Yan, H.; Chircov, C.; Zhong, X.; Winkeljann, B.; Dobryden, I.; Nilsson, H. E.; Lieleg, O.; Claesson, P. M.; Hedberg, Y.; Crouzier, T. Reversible Condensation of Mucins into Nanoparticles. *Langmuir* **2018**, *34* (45), 13615–13625.
- (13) Kuo, J. C. H.; Gandhi, J. G.; Zia, R. N.; Paszek, M. J. Physical Biology of the Cancer Cell Glycocalyx. *Nat. Phys.* **2018**, *14* (7), 658–669.
- (14) Arike, L.; Hansson, G. C. The Densely O-Glycosylated MUC2Mucin Protects the Intestine and Provides Food for the Commensal Bacteria. *J. Mol. Biol.* **2016**, *428* (16), 3221–3229.
- (15) Johansson, M. E. V.; Hansson, G. C. Immunological Aspects of Intestinal Mucus and Mucins. *Nat. Rev. Immunol.* **2016**, *16* (10), 639–649.
- (16) Shan, M.; Gentile, M.; Yeiser, J. R.; Walland, A. C.; Bornstein, V. U.; Chen, K.; He, B.; Cassis, L.; Bigas, A.; Cols, M.; Comerma, L.; Huang, B.; Blander, J. M.; Xiong, H.; Mayer, L.; Berin, C.; Augenlicht, L.; Velcich, A.; Cerutti, A. Mucus Enhances Gut Homeostasis and Oral Tolerance by Delivering Immunoregulatory Signals. *Science* **2013**, *342* (6157), 447–453.
- (17) Melo-Gonzalez, F.; Fenton, T. M.; Forss, C.; Smedley, C.; Goenka, A.; MacDonald, A. S.; Thornton, D. J.; Travis, M. A. Intestinal Mucin Activates Human Dendritic Cells and IL-8 Production in a Glycan-Specific Manner. *J. Biol. Chem.* **2018**, *293* (22), 8543–8553.
- (18) Kim, H. S.; Yoo, K. S.; Han, D. S. Gastric Invasion of the Intraductal Papillary Mucinous Tumor. *Video Journal and Encyclopedia of GI Endoscopy* **2013**, *1* (1), 170–171.
- (19) Inoue, M.; Fujii, H.; Kaseyama, H.; Yamashina, I.; Nakada, H. Stimulation of Macrophages by Mucins through a Macrophage Scavenger Receptor. *Biochem. Biophys. Res. Commun.* **1999**, *264* (1), 276–280.
- (20) Chung, L.; Maestas, D. R., Jr; Housseau, F.; Elisseeff, J. H. Key Players in the Immune Response to Biomaterial Scaffolds for Regenerative Medicine. *Adv. Drug Delivery Rev.* **2017**, *114*, 184–192.
- (21) Yan, H.; Seigne, C.; Hjorth, M.; Winkeljann, B.; Blakeley, M.; Lieleg, O.; Phillipson, M.; Crouzier, T. Immune-Informed Mucin Hydrogels Evade Fibrotic Foreign Body Response In Vivo. *Adv. Funct. Mater.* **2019**, *29*, 1902581.
- (22) Tarique, A. A.; Logan, J.; Thomas, E.; Holt, P. G.; Sly, P. D.; Fantino, E. Phenotypic, Functional, and Plasticity Features of Classical and Alternatively Activated Human Macrophages. *Am. J. Respir. Cell Mol. Biol.* **2015**, *53* (5), 676–688.
- (23) Chouaib, S.; Kieda, C.; Benlalam, H.; Noman, M. Z.; Mami-Chouaib, F.; Ruegg, C. Endothelial Cells as Key Determinants of the Tumor Microenvironment: Interaction with Tumor Cells, Extracellular Matrix and Immune Killer Cells. *Crit. Rev. Immunol.* **2010**, *30* (6), 529–545.
- (24) Janssen, W. J.; Stefanski, A. L.; Bochner, B. S.; Evans, C. M. Control of Lung Defence by Mucins and Macrophages: Ancient Defence Mechanisms with Modern Functions. *Eur. Respir. J.* **2016**, *48* (4), 1201–1214.
- (25) Blakney, A. K.; Swartzlander, M. D.; Bryant, S. J. The Effects of Substrate Stiffness on the in Vitro Activation of Macrophages and in Vivo Host Response to Poly(ethylene glycol)-Based Hydrogels. *J. Biomed. Mater. Res., Part A* **2012**, *100A* (6), 1375–1386.
- (26) Biegler, M.; Delius, J.; Käs Dorf, B. T.; Hofmann, T.; Lieleg, O. Cationic Astringents Alter the Tribological and Rheological Properties of Human Saliva and Salivary Mucin Solutions. *Biotribology* **2016**, *6*, 12–20.
- (27) Backes, S.; Von Klitzing, R. Nanomechanics and Nanorheology of Microgels at Interfaces. *Polymers* **2018**, *10* (9), 978.
- (28) Claesson, P. M.; Dobryden, I.; Li, G.; He, Y.; Huang, H.; Thorén, P.-A.; Haviland, D. B. From Force Curves to Surface Nanomechanical Properties. *Phys. Chem. Chem. Phys.* **2017**, *19* (35), 23642–23657.
- (29) Genin, M.; Clement, F.; Fattaccoli, A.; Raes, M.; Michiels, C. M1 and M2 Macrophages Derived from THP-1 Cells Differentially Modulate the Response of Cancer Cells to Etoposide. *BMC Cancer* **2015**, *15*, 577.
- (30) Mosser, D. M. The Many Faces of Macrophage Activation. *J. Leukocyte Biol.* **2003**, *73* (2), 209–212.
- (31) Recalcati, S.; Locati, M.; Marini, A.; Santambrogio, P.; Zaninotto, F.; De Pizzol, M.; Zammataro, L.; Girelli, D.; Cairo, G. Differential Regulation of Iron Homeostasis during Human Macrophage Polarized Activation. *Eur. J. Immunol.* **2010**, *40* (3), 824–835.
- (32) Mantovani, A.; Sica, A.; Sozzani, S.; Allavena, P.; Vecchi, A.; Locati, M. The Chemokine System in Diverse Forms of Macrophage Activation and Polarization. *Trends Immunol.* **2004**, *25* (12), 677–686.
- (33) Daigneault, M.; Preston, J. A.; Marriott, H. M.; Whyte, M. K. B.; Dockrell, D. H. The Identification of Markers of Macrophage Differentiation in PMA-Stimulated THP-1 Cells and Monocyte-Derived Macrophages. *PLoS One* **2010**, *5* (1), e8668.
- (34) Kuhl, P. R.; Griffith-Cima, L. G. Tethered Epidermal Growth Factor as a Paradigm for Growth Factor–induced Stimulation from the Solid Phase. *Nat. Med.* **1996**, *2* (9), 1022–1027.
- (35) Fourel, L.; Valat, A.; Faurobert, E.; Guillot, R.; Bourrin-Reynard, I.; Ren, K.; Lafanechère, L.; Planus, E.; Picart, C.; Albiges-Rizo, C. β 3 Integrin–mediated Spreading Induced by Matrix-Bound BMP-2 Controls Smad Signaling in a Stiffness-Independent Manner. *J. Cell Biol.* **2016**, *212* (6), 693–706.
- (36) Blache, U.; Stevens, M. M.; Gentleman, E. Harnessing the Secreted Extracellular Matrix to Engineer Tissues. *Nat. Biomed Eng.* **2020**, *4*, 357–363.
- (37) Kim, H.; Cha, J.; Jang, M.; Kim, P. Hyaluronic Acid-Based Extracellular Matrix Triggers Spontaneous M2-like Polarity of Monocyte/macrophage. *Biomater. Sci.* **2019**, *7* (6), 2264–2271.
- (38) Wang, H.; Morales, R. T. T.; Cui, X.; Huang, J.; Qian, W.; Tong, J.; Chen, W. A Photoresponsive Hyaluronan Hydrogel Nanocomposite for Dynamic Macrophage Immunomodulation. *Adv. Healthcare Mater.* **2018**, *8* (4), 1801234.
- (39) Court, M.; Malier, M.; Millet, A. 3D Type I Collagen Environment Leads up to a Reassessment of the Classification of Human Macrophage Polarizations. *Biomaterials* **2019**, *208*, 98–109.
- (40) Brinkman-Van der Linden, E. C. M.; Varki, A. New Aspects of Siglec Binding Specificities, Including the Significance of Fucosylation and of the Sialyl-Tn Epitope. *J. Biol. Chem.* **2000**, *275* (12), 8625–8632.
- (41) Tsuji, T.; Osawa, T. Carbohydrate structures of bovine submaxillary mucin. *Carbohydr. Res.* **1986**, *151*, 391–402.
- (42) Kim, J.; Lee, J.; Jang, Y.; Ha, J.; Kim, D.; Ji, M.; Lee, Y. K.; Kim, W.; You, S.; Do, J.; Ryu, C.; Kim, H. N-Glycans of Bovine Submaxillary Mucin Contain Core-Fucosylated and Sulfated Glycans but Not Sialylated Glycans. *Int. J. Biol. Macromol.* **2019**, *138*, 1072–1078.
- (43) Crocker, P. R.; Paulson, J. C.; Varki, A. Siglecs and Their Roles in the Immune System. *Nat. Rev. Immunol.* **2007**, *7* (4), 255–266.
- (44) Varki, A.; Gagneux, P. Multifarious roles of sialic acids in immunity. *Ann. N. Y. Acad. Sci.* **2012**, *1253*, 16–36.
- (45) Crocker, P. R.; Varki, A. Siglecs, sialic acids and innate immunity. *Trends Immunol.* **2001**, *22*, 337–342.
- (46) Lübbers, J.; Rodríguez, E.; van Kooyk, Y. Modulation of Immune Tolerance via Siglec-Sialic Acid Interactions. *Front. Immunol.* **2018**, *9*, 2807.
- (47) Forrester, M. A.; Wassall, H. J.; Hall, L. S.; Cao, H.; Wilson, H. M.; Barker, R. N.; Vickers, M. A. Similarities and Differences in Surface Receptor Expression by THP-1 Monocytes and Differentiated Macrophages Polarized Using Seven Different Conditioning Regimens. *Cell. Immunol.* **2018**, *332*, 58–76.
- (48) Lock, K.; Zhang, J.; Lu, J.; Lee, S. H.; Crocker, P. R. Expression of CD33-Related Siglecs on Human Mononuclear Phagocytes, Monocyte-Derived Dendritic Cells and Plasmacytoid Dendritic Cells. *Immunobiology* **2004**, *209* (1–2), 199–207.
- (49) Brinkman-Van der Linden, E. C. M.; Angata, T.; Reynolds, S. A.; Powell, L. D.; Hedrick, S. M.; Varki, A. CD33/Siglec-3 Binding Specificity, Expression Pattern, and Consequences of Gene Deletion in Mice. *Mol. Cell. Biol.* **2003**, *23* (12), 4199–4206.
- (50) Blixt, O.; Collins, B. E.; van den Nieuwenhof, I. M.; Crocker, P. R.; Paulson, J. C. Sialoside Specificity of the Siglec Family Assessed Using Novel Multivalent Probes: Identification of Potent Inhibitors of Myelin-Associated Glycoprotein. *J. Biol. Chem.* **2003**, *278* (33), 31007–31019.

- (51) Angata, T.; Tabuchi, Y.; Nakamura, K.; Nakamura, M. Siglec-15: An Immune System Siglec Conserved throughout Vertebrate Evolution. *Glycobiology* **2007**, *17* (8), 838–846.
- (52) Ohta, M.; Ishida, A.; Toda, M.; Akita, K.; Inoue, M.; Yamashita, K.; Watanabe, M.; Murata, T.; Usui, T.; Nakada, H. Immunomodulation of Monocyte-Derived Dendritic Cells through Ligation of Tumor-Produced Mucins to Siglec-9. *Biochem. Biophys. Res. Commun.* **2010**, *402* (4), 663–669.
- (53) Chen, G.-Y.; Brown, N. K.; Wu, W.; Khedri, Z.; Yu, H.; Chen, X.; van de Vlekkert, D.; D'Azzo, A.; Zheng, P.; Liu, Y. Broad and Direct Interaction between TLR and Siglec Families of Pattern Recognition Receptors and Its Regulation by Neu1. *eLife* **2014**, *3*, e04066.
- (54) Macauley, M. S.; Crocker, P. R.; Paulson, J. C. Siglec-Mediated Regulation of Immune Cell Function in Disease. *Nat. Rev. Immunol.* **2014**, *14* (10), 653–666.
- (55) Beatson, R.; Tajadura-Ortega, V.; Achkova, D.; Picco, G.; Tsourouktsoglou, T.-D.; Klausing, S.; Hillier, M.; Maher, J.; Noll, T.; Crocker, P. R.; Taylor-Papadimitriou, J.; Burchell, J. M. The Mucin MUC1 Modulates the Tumor Immunological Microenvironment through Engagement of the Lectin Siglec-9. *Nat. Immunol.* **2016**, *17* (11), 1273–1281.
- (56) Crocker, P. R.; McMillan, S. J.; Richards, H. E. CD33-Related Siglecs as Potential Modulators of Inflammatory Responses. *Ann. N. Y. Acad. Sci.* **2012**, *1253* (1), 102–111.
- (57) Sahin, O.; Mandriota, N.; Molina, J. J.; Tatem, K. Relating Local Nanomechanical Response of Cells to Intracellular Forces and Cell Morphology. *Biophys. J.* **2015**, *108* (2), 140a.
- (58) Doloff, J. C.; Veisheh, O.; Vegas, A. J.; Tam, H. H.; Farah, S.; Ma, M.; Li, J.; Bader, A.; Chiu, A.; Sadraei, A.; Aresta-Dasilva, S.; Griffin, M.; Jhunjhunwala, S.; Webber, M.; Siebert, S.; Tang, K.; Chen, M.; Langan, E.; Dholokia, N.; Thakrar, R.; Qi, M.; Oberholzer, J.; Greiner, D. L.; Langer, R.; Anderson, D. G. Colony Stimulating Factor-1 Receptor Is a Central Component of the Foreign Body Response to Biomaterial Implants in Rodents and Non-Human Primates. *Nat. Mater.* **2017**, *16* (6), 671–680.
- (59) Jhunjhunwala, S. Neutrophils at the Biological–Material Interface. *ACS Biomater. Sci. Eng.* **2018**, *4* (4), 1128–1136.
- (60) Ode Boni, B. O.; Lamboni, L.; Souho, T.; Gauthier, M.; Yang, G. Immunomodulation and Cellular Response to Biomaterials: The Overriding Role of Neutrophils in Healing. *Mater. Horiz.* **2019**, *6* (6), 1122–1137.
- (61) Lee, K. Y.; Mooney, D. J. Alginate: Properties and Biomedical Applications. *Prog. Polym. Sci.* **2012**, *37* (1), 106–126.
- (62) Yamanlar, S.; Sant, S.; Boudou, T.; Picart, C.; Khademhosseini, A. Surface Functionalization of Hyaluronic Acid Hydrogels by Polyelectrolyte Multilayer Films. *Biomaterials* **2011**, *32* (24), 5590–5599.
- (63) Crouzier, T.; Jang, H.; Ahn, J.; Stocker, R.; Ribbeck, K. Cell Patterning with Mucin Biopolymers. *Biomacromolecules* **2013**, *14* (9), 3010–3016.
- (64) van der Poel, C. E.; Spaapen, R. M.; van de Winkel, J. G. J.; Leusen, J. H. W. Functional Characteristics of the High Affinity IgG Receptor, FcγRI. *J. Immunol.* **2011**, *186* (5), 2699–2704.
- (65) Azad, A. K.; Rajaram, M. V. S.; Schlesinger, L. S. Exploitation of the Macrophage Mannose Receptor (CD206) in Infectious Disease Diagnostics and Therapeutics. *J. Cytol. Mol. Biol.* **2014**, *1* (1), 1000003.
- (66) Kato, K.; Uchino, R.; Lillehoj, E. P.; Knox, K.; Lin, Y.; Kim, K. C. Membrane-Tethered MUC1 Mucin Counter-Regulates the Phagocytic Activity of Macrophages. *Am. J. Respir. Cell Mol. Biol.* **2016**, *54* (4), 515–523.
- (67) Mosser, D. M.; Edwards, J. P. Exploring the Full Spectrum of Macrophage Activation. *Nat. Rev. Immunol.* **2008**, *8* (12), 958–969.
- (68) Mooney, J. E.; Summers, K. M.; Gongora, M.; Grimmond, S. M.; Campbell, J. H.; Hume, D. A.; Rolfe, B. E. Transcriptional Switching in Macrophages Associated with the Peritoneal Foreign Body Response. *Immunol. Cell Biol.* **2014**, *92* (6), 518–526.
- (69) Saeland, E.; van Vliet, S. J.; Bäckström, M.; van den Berg, V. C. M.; Geijtenbeek, T. B. H.; Meijer, G. A.; van Kooyk, Y. The C-Type Lectin MGL Expressed by Dendritic Cells Detects Glycan Changes on MUC1 in Colon Carcinoma. *Cancer Immunol. Immunother.* **2007**, *56* (8), 1225–1236.
- (70) Ju, T.; Otto, V. I.; Cummings, R. D. The Tn Antigen-Structural Simplicity and Biological Complexity. *Angew. Chem., Int. Ed.* **2011**, *50* (8), 1770–1791.
- (71) Shahraz, A.; Kopatz, J.; Mathy, R.; Kappler, J.; Winter, D.; Kapoor, S.; Schütza, V.; Scheper, T.; Gieselmann, V.; Neumann, H. Anti-Inflammatory Activity of Low Molecular Weight Polysialic Acid on Human Macrophages. *Sci. Rep.* **2015**, *5*, 16800.
- (72) Li, G.; Dobryden, I.; Salazar-Sandoval, E. J.; Johansson, M.; Claesson, P. M. Load-Dependent Surface Nanomechanical Properties of Poly-HEMA Hydrogels in Aqueous Medium. *Soft Matter* **2019**, *15* (38), 7704–7714.